Successful KickFlip: Dynamic Analysis and Influencing Factors of the Skateboard KickFlip Motion

Yuchen Zhong

Chongqing BI Academy, Chongqing 401120, China

Abstract

This paper studies the Flick action in skateboarding by constructing a rigid-body dynamics model of the skateboard's airborne motion and combining it with measured data from the MPU6050 inertial measurement unit (IMU). In the experiment, a miniature skateboard equipped with an MPU6050 was used to measure angular velocity and attitude angles during flipping. In the theory part, a coordinate system with the skateboard's center of mass as the origin was established, the torques about the X and Y axes caused by the Flick force were derived, and the variation law of the skateboard's flipping attitude in the air was numerically simulated. By comparing the simulation with measured data, the rationality of the model was verified and the sources of error were discussed. The results show that the theoretical model can better predict the roll flipping trend about the skateboard's longitudinal axis (X axis), and the error between the simulated curve and the experimental curve is controlled within ±5%.

Keywords

Skateboard, KickFlip, attitude, moment of inertia, Rigid-body dynamics.

1. Introduction

As an extreme sport integrating competitiveness, entertainment, and technical skill, skateboarding occupies an important place not only in recreation and street culture but has also recently been included as an official Olympic event, further promoting its technical development and scientific training needs [1]. However, skateboarding is highly dependent on experience and muscle memory. Mastering a trick often requires extensive practice and repeated failure. As a national second-level skateboard athlete, I often wondered during daily training whether physics could be used to analyze skateboard motion more precisely, thereby providing quantitative guidance for action improvement and accelerating training progress. Based on this idea, the following research was conducted.

Although there are many types of skateboard tricks, most are derived from basic movements such as Ollie, KickFlip, and Heelflip. These tricks depend on the athlete's ability to control the instantaneous attitude of the skateboard in the air. Precise airborne control requires both appropriate force application and timing. This study focuses on the KickFlip, in which the rider flicks the edge of the board with the toe during ascent, causing the board to rotate longitudinally about its long axis. This motion is fundamental to many advanced tricks.

While practicing this trick, a mathematical model was established to describe the attitude evolution and dynamic characteristics of the skateboard. A local coordinate system centered at the center of mass was defined, and moments of inertia around different axes were calculated. By analyzing the direction and point of application of the flick force, the external torque expression was constructed. Combined with the relationship between Euler angles and angular velocity, numerical integration was used to simulate roll, pitch, and yaw evolution over time.

Since the skateboard is an irregular object with nonuniform mass distribution and short-duration impulsive forces, modeling errors are inevitable. Therefore, experimental data were

collected for calibration. A small skateboard model equipped with an MPU6050 IMU was designed. Angular velocity and acceleration data during flight were recorded. Because accelerometer data are strongly affected by centrifugal, Coriolis, and gravitational variations during dynamic motion, gyroscope data were used as the primary basis for attitude estimation.

Simulation results were compared with measured angular velocity data. After incorporating rebound force modeling and parameter optimization, strong agreement was achieved, especially for roll motion around the X axis. This demonstrates the validity and applicability of the proposed modeling approach.

This study establishes a quantitative dynamic modeling framework for airborne kickflip motion and provides a foundation for trick recognition, technique evaluation, and motion capture system development.

2. Basic Theoretical Model

During the complete process of performing a kickflip, the skateboard is mainly subjected to two forces. The first is the force that makes the skateboard pop up, which comes from the rider's "pop" action at the ankle after jumping, causing the tail of the board to strike the ground, generating a rebound force that pushes the board upward. The other force is the "flick force" produced when the rider kicks the side of the skateboard with the toe during the board's upward motion, and this force is the main cause of the board's longitudinal flip. In analysis, this flick force can be regarded as acting perpendicular to the skateboard, denoted as fkickflip.

The rebound force originates from the more fundamental ollie, which only produces a vertical force to lift the board and provides a tilt angle, and it is not strongly related to the flipping motion. Therefore, the rebound force is not analyzed in detail here, and instead the skateboard's initial height, tilt angle, and initial velocity are treated as boundary conditions, with emphasis on analyzing the flip after the board is subjected to the flick force in the air, while ignoring small forces such as air resistance.

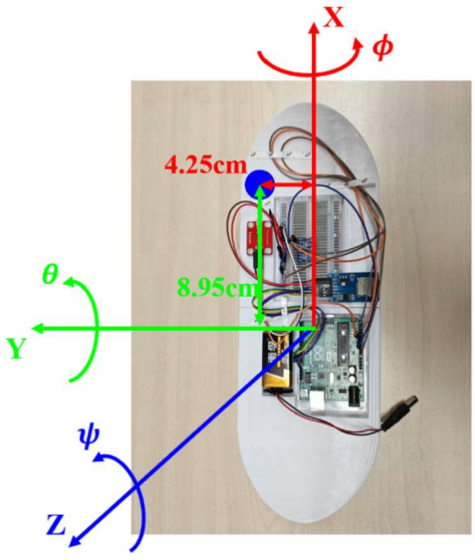

Figure 1. Skateboard coordinate system and force application point location

A local coordinate system for the skateboard is established, as shown in figure 1. During airborne flight, terms commonly used to describe aircraft attitude are adopted, using roll, pitch, and yaw angles to describe the skateboard's attitude in the air.

The rotation direction of attitude angles follows the right-hand rule, where the thumb points to the positive direction of the axis, and the direction of the other four fingers indicates the

positive direction of the attitude angle. Attitude angles are essentially a set of parameters describing the transformation between the skateboard local coordinate system and the global coordinate system, and the rotation matrices used for the transformation are shown in equations (1) to (3). The derivation is lengthy, and details are provided in appendix 1.

The motion of the skateboard is governed by newtonian mechanics, and here it is mainly influenced by newton's second law, namely

$$R_z(\psi) = \begin{bmatrix} cos\psi & -sin\psi & 0 \\ sin\psi & cos\psi & 0 \\ 0 & 0 & 1 \end{bmatrix} \tag{1}$$

$$R_y(\theta) = \begin{bmatrix} cos\theta & 0 & sin\theta \\ 0 & 1 & 0 \\ -sin\theta & 0 & cos\theta \end{bmatrix} \tag{2}$$

$$R_x(\phi) = \begin{bmatrix} 1 & 0 & 0 \\ 0 & cos\phi & -sin\phi \\ 0 & sin\phi & cos\phi \end{bmatrix} \tag{3}$$

The motion of the skateboard is governed by newtonian mechanics, and here it is mainly influenced by newton's second law, namely

$$F = ma \tag{4}$$

Here, newton's second law is manifested not only in translation but also in rotational motion about the skateboard axes.

The skateboard is approximated as a rectangular plate structure, and a local coordinate system is established on its upper surface, as shown in figure 2.

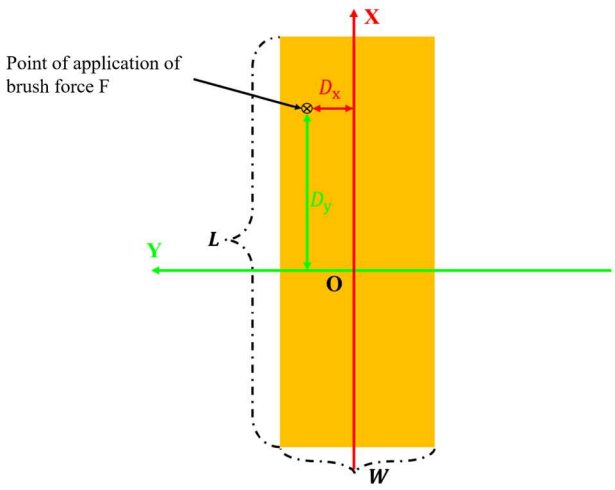

Figure 2. Schematic of skateboard local coordinate system

Skateboard rotation also follows newton's second law. Note that the flick force application point has distances from both the x axis and y axis, meaning that this force will produce at least two torque components. In fact, when performing a kickflip, the ankle's kick at the nose also

produces friction, meaning a yaw angle about the z axis may also occur, but in the current analysis, this force is simplified as a vertical force, so only the two torque components producing pitch and roll are considered.

An explicit numerical model is used for theoretical calculation, with the process shown in figure 3. First, compute the torque generated by the flick force within time t, which produces angular acceleration, then update angular velocity and euler angles, and then determine whether the flick force still acts at the next time step.

If the flick force still exists, compute the 3d full rotation matrix within time t from the euler angles, and update the action vector of the flick force.

If the flick force disappears, then there is no torque, and neglecting air resistance, angular acceleration becomes zero, angular velocity remains constant, and euler angles are continuously updated until time stepping ends.

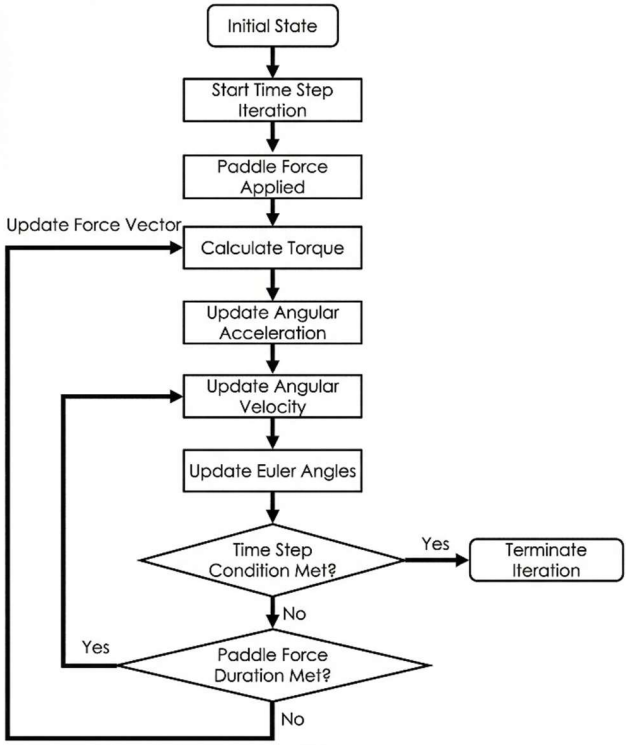

Figure 3. Theoretical analysis flowchart

The torque calculation is[4]

$$\tau = F \cdot D \tag{5}$$

In the equation, D is the moment arm, and since the force is vertical, the moment arm is the perpendicular distance from the flick force application point to the X axis and Y axis.

Angular acceleration is given by equation (6)

$$\alpha = \tau / I \tag{6}$$

In the equation, I is the moment of inertia.

To calculate the moments of inertia of a rectangular plate about its central long axis and short axis, we first set the coordinate system so that the plate center is at the origin, the short side is along the X axis, and the long side is along the Y axis.

The rectangle's length and width are L and W, and mass is M, so the density is

$$\sigma = \frac{M}{LW} \tag{7}$$

The moment of inertia I_x about the x axis is given by the integral formula

$$I_x = \int r^2 \, dm \tag{8}$$

Here, the distance to the X axis is y, so the integral becomes

$$I_x = \sigma \int_{-W/2}^{W/2} \int_{-L/2}^{L/2} y^2 \, dy \, dx \tag{9}$$

Since the integrand is independent of x, the integral can be separated

$$I_x = \sigma \left(\int_{-W/2}^{W/2} dx \right) \left(\int_{-L/2}^{L/2} y^2 \, dy \right) \tag{10}$$

Compute the integral

$$\int_{-W/2}^{W/2} dx = W \tag{11}$$

$$\int_{-L/2}^{L/2} y^2 dy = 2 \int_{0}^{L/2} y^2 dy = \frac{L^3}{12} \tag{12}$$

Substituting equation (7) yields the moment of inertia about the X axis (central short axis)

$$I_x = \frac{M}{LW} \cdot W \cdot \frac{L^3}{12} = \frac{ML^2}{12} \tag{13}$$

Similarly, the moment of inertia about the Y axis (central long axis) is

$$I_y = \frac{MW^2}{12} \tag{14}$$

Combining equations (5) and (14), the angular accelerations along X and Y axes can be obtained

$$\alpha_x = \tau_x / I_x \tag{15}$$

$$\alpha_y = \tau_y / I_y \tag{16}$$

After obtaining angular acceleration, double integration gives the corresponding attitude angles

$$\phi = \iint \alpha_x \, dt \tag{17}$$

$$\theta = \iint \alpha_y \, dt \tag{18}$$

The full rotation matrix derived from attitude angles is used to update the coordinate representation of the flick force vector, and the iteration continues. Using python for theoretical modeling, with code shown in appendix 2, the skateboard's airborne attitude can be simulated.

3. Experimental Apparatus and Attitude Estimation

3.1. Experimental Apparatus

The overall experimental architecture is shown in Figure 4. The basic principle of the experimental apparatus is shown in Figure 5a, and the physical setup is shown in Figure 5b. The small skateboard model is a plastic part made by 3D printing, with thickness kept as close as possible to a real skateboard, and multiple measurement components are integrated on the back of the model. The layout positions of components are adjusted to keep the integrated center of mass as close as possible to the geometric center of the skateboard. A flipping torque is applied by the flick force F at the application point, the FSR pressure sensor records the magnitude of applied force F, and the MPU6050 records the three-axis acceleration and angular velocity during the experiment. All measurement data are written to an SD card by an Arduino microcontroller, and after the experiment, SD card data are read for attitude estimation to obtain attitude angles. The Arduino code for reading measurement data is shown in Appendix 3. [5] The compiler used is Arduino IDE.

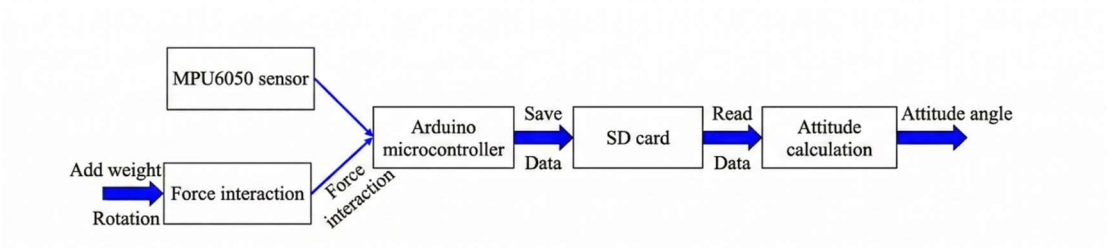

Figure 4. Overall experimental architecture

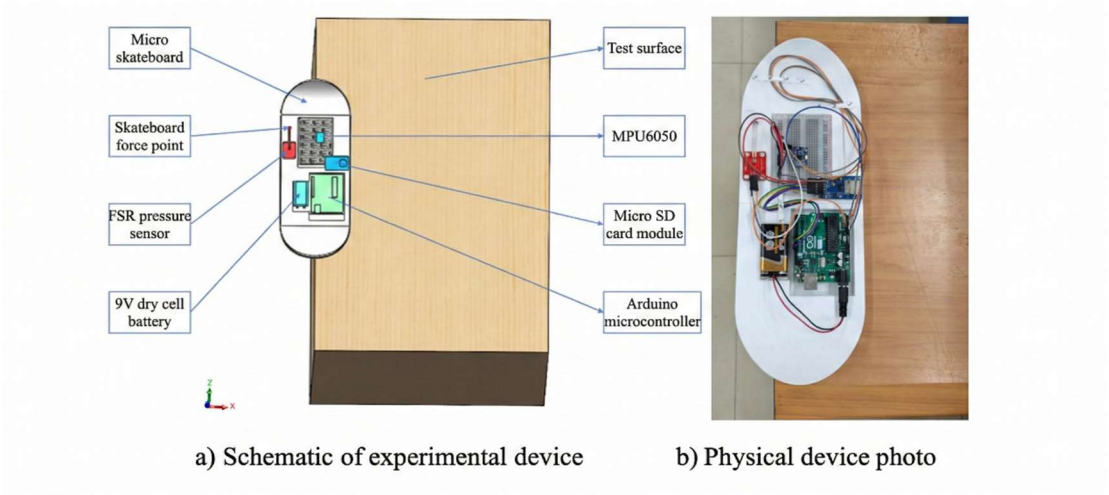

Figure 5. Experimental apparatus

While the skateboard flips, a phone camera (60 FPS) is used to record video, and then the video is slowed down with editing software and analyzed together with measured data to study the airborne attitude.

The main sensor accuracy and measurement ranges in this experiment are shown in Table 1. During the experiment, some variables are kept constant, and their values are shown in Table 2.

Table 1. Measurement ranges and accuracy of tools

Variable name	Measurement tool model	Measurement range / measurement accuracy
Three-axis acceleration(g)	MPU6050 six-axis sensor	±16(±0.09)
Three-axis angular velocity (°/s)	MPU6050 six-axis sensor	±2000(±1.5)
Flick force (kg)	FSR pressure sensor	0-5 (±0.1)
Weight (kg)	Electronic scale	0-10 (±0.001)
Time (s)	Arduino microcontroller	0-3600 (±0.025)
Length (cm)	Vernier caliper	0-15 (±0.05)

Table 2. Fixed variables

Variable name	Value
Test table height (mm)	644
Equivalent skateboard length (mm)	303.72
Skateboard width (mm)	120
Total weight of skateboard model (g)	300

3.2. Experimental Results and Preliminary Analysis

A pre-experiment was conducted under the above conditions.

To preliminarily verify the flipping motion characteristics of the airborne skateboard under force, a pre-experiment was first performed with flick force application point coordinates [0.0895, 0.0425, 0] (unit: m) and F = 5 N.

This application point lies in the first quadrant and will produce a torque mainly causing flipping about the X axis (long axis).

In the experiment, the skateboard's attitude states at different times during flight were collected.

Figure 6 shows frames at moments when the skateboard's roll angle about the X axis reaches −90°, −180°, −270°, and −360°.

Image analysis indicates that the airborne trajectory is approximately parabolic, and the attitude angles change roughly linearly with time.

At the moment of landing, the roll, pitch, and yaw angles are approximately −360°, +10°, and −30°.

Before analyzing experimental data measured by the MPU6050, first observe its readings in a stationary state, as shown in Figure 7.

From Figure 7a, the Z direction has an initial acceleration of 1.09 g, the Y direction has 0.09 g, and the X direction is 0.

Normally, the Z direction should read 1 g due to gravity and the Y direction should be 0, indicating that when the sensor is stationary, noise causes about 0.09 g bias.

Throughout the stationary period, fluctuations in all three accelerations are very small and stable.

From Figure 7b, under Earth's magnetic field influence, the angular velocity has a bias of about ±1.5 °/s when the sensor is stationary and level, and the overall trend is also stable.
The MPU6050 readings can be considered reasonably accurate and stable.

Figure 6. Decomposition of experimental phenomenon (skateboard moves from right to left)

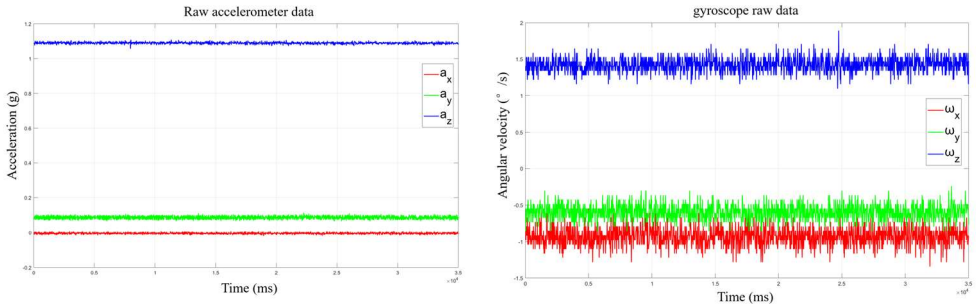

a) Acceleration b) Angular velocity

Figure 7. MPU6050 data recording at rest

Figure 7. shows the data corresponding to the phenomenon in Figure 6. From Figure 7a, as rotation proceeds, accelerations in X, Y, and Z change greatly, especially in Y and Z. The main reason is that during rotation about the X axis, the axis orientation changes significantly, for example, initially the vertical direction is the Z axis, at 0.11 s the vertical direction becomes the Y axis, and at 0.22 s it becomes the Z axis again.
In addition, during rotation there are centrifugal acceleration terms, Coriolis acceleration terms (usually small and can be ignored), and Euler acceleration terms, all of which cause severe acceleration variation.
Therefore, the accelerometer is inaccurate in dynamic processes.

$$\vec{a} = \vec{a}_{measure} - \vec{\omega} \times (\vec{\omega} \times \vec{r}) - \vec{\alpha} \times \vec{r} \tag{19}$$

In the equation, $\vec{\omega}$ is angular velocity, $\vec{r}$ is the position vector of the accelerometer relative to the center of mass, $\vec{\alpha}$ and is angular acceleration.
The first term $\vec{a}_{measure}$ is the accelerometer's direct measurement, the second term $\vec{\omega} \times (\vec{\omega} \times \vec{r})$ is centrifugal acceleration, and the third term $\vec{\alpha} \times \vec{r}$ is Euler acceleration.
From Figure 7b, angular velocities along Y and Z do not change much, while the X-axis angular velocity changes drastically and shows an obvious negative value, corresponding to roll being

about −360° at landing, with pitch and yaw changing less, which matches the observed phenomenon.

Therefore, the gyroscope is relatively accurate in dynamic processes.

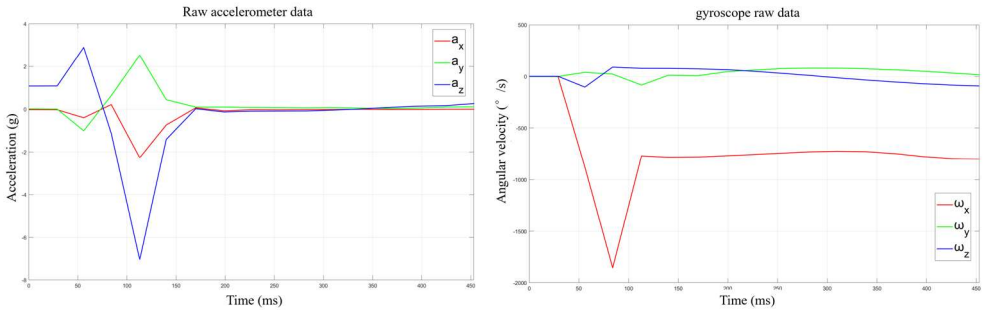

a) Acceleration b) Angular velocity

Figure 8. MPU6050 experimental data recording

3.3. Attitude Estimation

In Section 3.2, measured acceleration and angular velocity were obtained, but these alone cannot directly determine the object's attitude. This is because the gyroscope alone cannot provide angle, only angular velocity.

The accelerometer is not accurate in dynamics and is disturbed by linear motion and centrifugal forces. Therefore, to obtain attitude angles during motion, mathematical processing of the raw data is needed, namely attitude estimation.[6]

3.3.1. Accelerometer Attitude Estimation

From Figure 7a, when the MPU6050 is placed stationary and level, the Z-axis acceleration is 1 g, and X and Y accelerations are 0 (ignoring stationary noise), which can be written as the vector (0, 0, g). When the accelerometer is rotated to a certain attitude, gravitational acceleration produces components on the three axes, which is essentially the coordinate of (0, 0, g) in the Earth frame expressed in the accelerometer's own frame after rotation, as shown in Figure 9. The three readings are the transformed (0, 0, g) vector. [2]

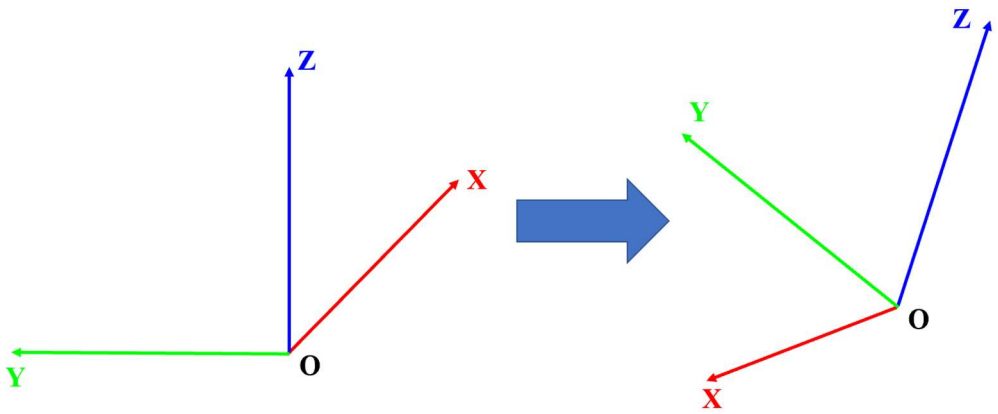

Figure 9. Change of accelerometer coordinate system

The attitude rotation is obtained in ZYX order, and the derivation of the full rotation matrix Mzyx is given in Appendix 1.

$$\begin{bmatrix} a_x \\ a_y \\ a_z \end{bmatrix} = M_{ZYX} \begin{bmatrix} 0 \\ 0 \\ g \end{bmatrix} = \begin{bmatrix} -sin\theta \\ cos\theta \cdot sin\phi \\ cos\theta \cdot cos\phi \end{bmatrix} \begin{bmatrix} 0 \\ 0 \\ g \end{bmatrix} \tag{20}$$

Solving Equation (20) yields roll and pitch angles. Since gravity does not change under rotation about the Z axis, accelerometer attitude estimation cannot compute yaw.

$$roll = \arctan\left(a_y / a_z\right) \tag{21}$$

$$pitch = -\arctan(a_x / \sqrt{{a_y}^2 + {a_z}^2}) \tag{22}$$

3.3.2. Gyroscope Attitude Estimation

A gyroscope is defined as measuring angular velocity about three axes, so integrating gyroscope data yields angles.

As in Figure 9, let the left coordinate system be at time i and the right be at time i+1, then the attitude angles at time i+1 can be expressed as $\phi + \Delta\phi$, $\theta + \Delta\theta$, $\psi + \Delta\psi$, and the angle increments can be expressed as

$$\begin{cases} \Delta\phi = \frac{d\phi}{dt}\Delta t \\ \Delta\theta = \frac{d\theta}{dt}\Delta t \\ \Delta\psi = \frac{d\psi}{dt}\Delta t \end{cases} \tag{23}$$

Attitude estimation is

$$\begin{cases} roll(i+1) = roll(i) + \frac{d\phi}{dt}\Delta t \\ pitch(i+1) = roll(i) + \frac{d\theta}{dt}\Delta t \\ yaw(i+1) = roll(i) + \frac{d\psi}{dt}\Delta t \end{cases} \tag{24}$$

3.3.3. Sensor Fusion Attitude Estimation

Sensor fusion combines the accelerometer's static stability and the gyroscope's dynamic stability, avoiding accelerometer dynamic disturbance and gyroscope integration drift. [7] Common fusion algorithms include the complementary filter and the Kalman filter. Their reliability in this experimental model was compared, as shown in Figure 10. From Figure 10c, residuals of both filters are less than 2.5°, indicating consistent overall trends. In the complementary filter result, roll is −341.3° and pitch is 14.7°. In the Kalman filter result, roll is −339.3° and pitch is 15.3°. According to the experimental phenomenon in Figure 6, at landing roll and pitch are approximately −360° and +10°, so the complementary filter is closer to the video observation.

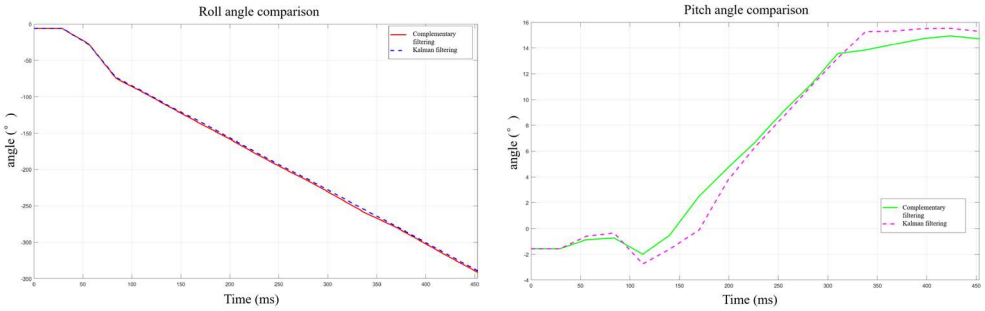

a) roll b) pitch

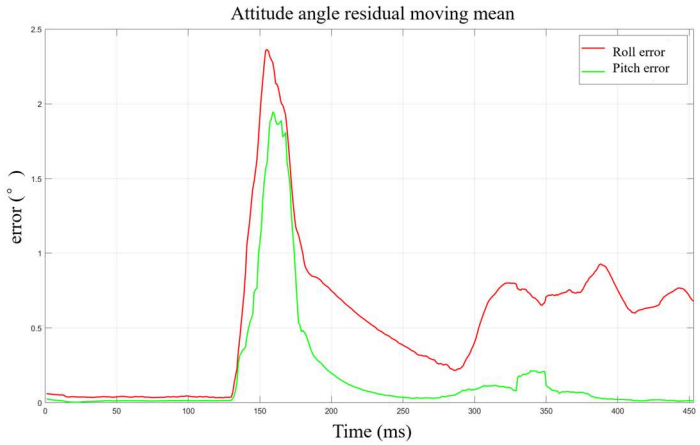

c) Comparison of attitude angle residuals

Figure 10. Comparison of sensor fusion attitude estimation

The complementary filter can be understood as choosing a value α between 0 and 1 to decide whether to trust the accelerometer more or the gyroscope more. The expression is as follows (since the accelerometer cannot obtain yaw, only roll and pitch are fused)

$$\begin{cases} roll = \alpha \cdot roll_{gryo} + (1-\alpha) \cdot roll_{acc} \\ pitch = \alpha \cdot pitch_{gryo} + (1-\alpha) \cdot pitch_{acc} \\ yaw = yaw_{gryo} \end{cases} \tag{25}$$

In the equation, gyro denotes the gyroscope estimation value, acc denotes the accelerometer estimation value, and in this study α is set to 0.96, with code shown in Appendix 4. The Kalman filter is another fusion approach. The overall Kalman result used here is actually obtained by applying complementary fusion once more between the gyroscope Kalman result and the accelerometer Kalman result, with α still 0.96.

Theoretically, Kalman filtering should perform better than direct complementary filtering, but in actual tests the Kalman result was not ideal, possibly because the process noise covariance matrix Q and measurement noise covariance matrix R were not accurately chosen. Therefore, the complementary filter result is used as the final test result.[3]

4. Results Analysis and Comparison

4.1. Theoretical Model Correction

After obtaining experimental data, a comparative analysis with the basic theoretical model derived in Section 2 was performed, as shown in Figure 11.

Figure 11a compares theoretical and experimental angular velocities in X and Y directions, showing that the current theory does not reproduce the trend where X-axis angular velocity

rapidly decreases and then rises, and Y-axis angular velocity differs significantly from experiment.

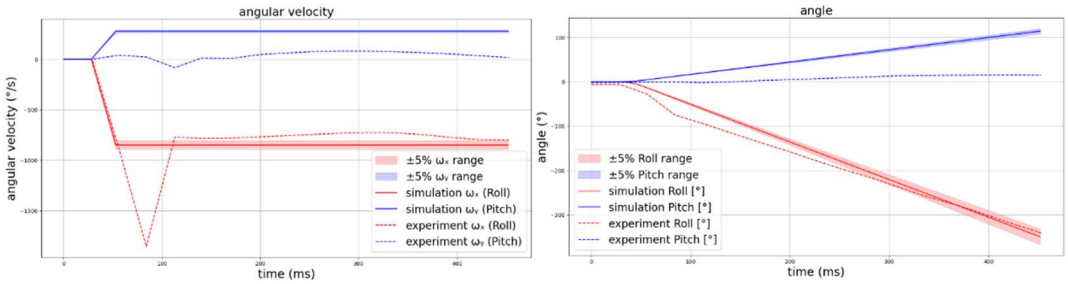

a) Angular velocity b) Attitude angle

Figure 11. Comparative analysis of theoretical and experimental results

Figure 11b compares attitude angles, showing that the theoretical roll about the X axis has small error relative to experiment, but pitch about the Y axis still has large deviation. The reason relates to experimental initial conditions. Theoretically, after force application, a pitch angular acceleration about Y should appear immediately, but in the experiment the board rolls off the table edge downward, initially blocked by the table surface, so initial pitch velocity cannot form, causing larger subsequent error.

In the theoretical attitude calculation, the Y-axis degree of freedom was not constrained. After obtaining measured angular velocity data, combined with experimental images, the Y-axis torque during the interval from when the flick force begins to act until the skateboard leaves the table was constrained.

In the previous theoretical analysis, only a downward flick force F was considered, so once the flick ends, angular velocity remains constant.However, the experimental results show a rising trend. A possible physical reason is that after the flick force is removed, there exists an opposite rebound torque that increases angular velocity and causes the rise. This may be because the skateboard is 3D printed and the material has elasticity, storing elastic potential energy during the flick, and releasing it after the flick ends to produce a torque about the X axis.

Including the Y-axis torque constraint and the rebound model to correct the theoretical model yields the comparison in Figure 12. It can be seen that after correction, the error between the theoretical model and experimental results is within ±5% for both angular velocity and attitude angle.

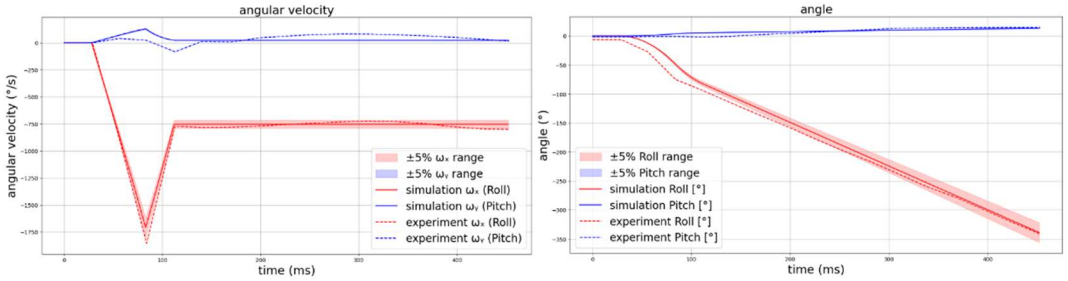

a) Angular velocity b) Attitude angle

Figure 12. Comparison of corrected theoretical and experimental results

Then another experiment was conducted to verify repeatability of the corrected model, with the same application point [0.0895, 0.0425, 0] (m) and F = 2.2 N.

The physical frames are shown in Figure 13, and the comparison is shown in Figure 14. It can be seen that for both angular velocity and attitude angle, the theoretical model has small error relative to experiment, proving the reliability of the corrected model.

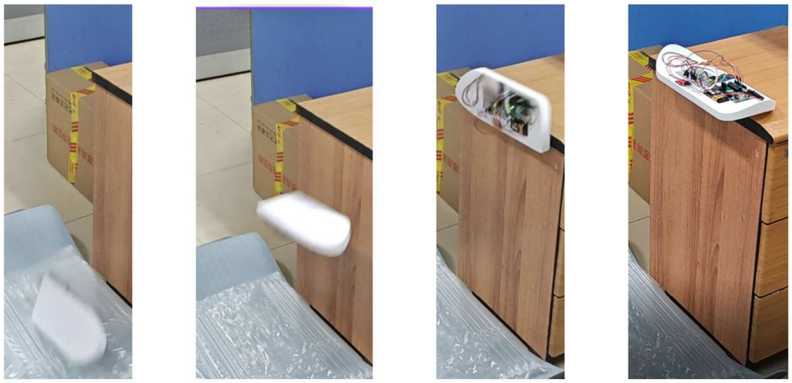

Figure 13. Decomposition of repeated experimental phenomenon (skateboard moves from right to left)

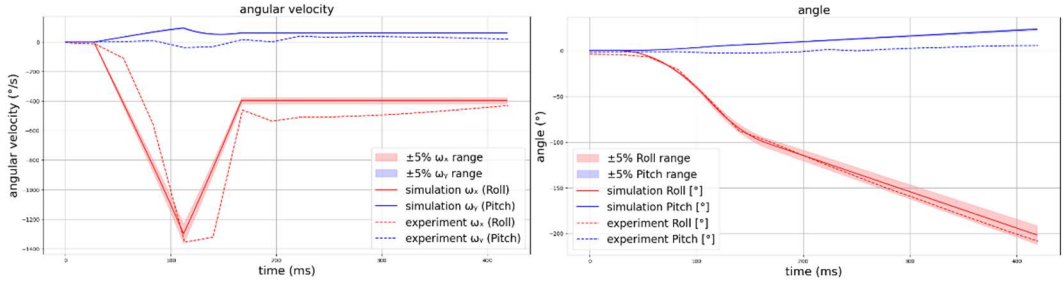

a) Angular velocity b) Attitude angle

Figure 14. Repeatability test of corrected theoretical results

4.2. Factors Affecting Airborne Attitude

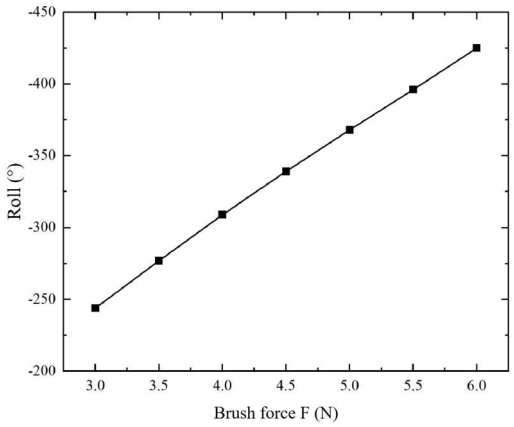

Figure 15. Effect of flick force magnitude on roll angle

Based on the corrected model, the main factors affecting airborne attitude include the magnitude of flick force F, the application position, and the force vector direction.

Their effects on roll are studied in order, while keeping other factors unchanged when analyzing a single factor.

The effect of flick force magnitude on roll is shown in Figure 15.

As F increases, roll increases in the negative direction, meaning larger F produces more rotation in the air.

The effect of changing the distance of the force application point to axes on roll is shown in Figure 16. The horizontal axis indicates the change of the application point distance to the coordinate axes. Initially X is 89.5 mm and Y is 42.5 mm, and as the horizontal axis increases, the application point coordinates increase. It is clear that changes in the Y coordinate have a much larger effect on roll than changes in X. Coordinate changes alter torque, and under the same coordinate change, the relative change rate in Y is larger, leading to a larger torque increase. Also, since the moment of inertia about X is smaller than that about Y, angular acceleration is larger, causing a larger roll change.

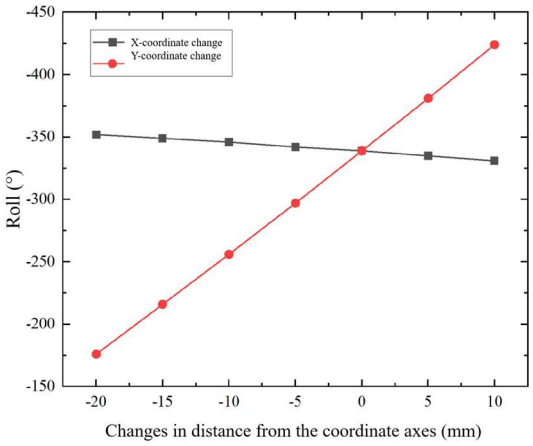

Figure 16. Effect of application point distance change on roll angle

The effect of the flick force vector on roll is shown in Figure 17.

Initially the vector is [0, 0, -1]. As the force vector increases, roll first increases and then decreases. It can also be seen that the influences of X and Y vector components differ. When the vector changes in the negative direction, the X component influence is more obvious. When the vector changes in the positive direction, the Y component influence is more obvious. When the vector is [0, 0, -1], the roll angle is maximal, namely -339°.

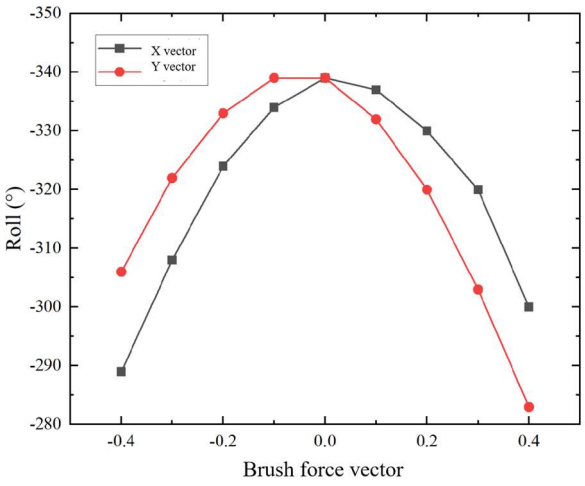

Figure 17. Effect of flick force vector on roll angle

4.3. Optimization Analysis

The purpose of this experiment is to simulate the real skateboard flight attitude.

In a real KickFlip, the skateboard does not complete a full 360° roll at the moment of landing, but completes it before both feet land on the board.

That is, a good KickFlip should complete one full rotation before the feet land back on the board. For this experiment, total duration is 0.453 s and flick force starts at 0.029 s. Considering an airborne time of 0.3 s after the feet leave the board, if at time 0.329 s the roll angle is close to -360°, it can be considered a perfect flip. Based on the factor analysis above, when only changing F magnitude, when F = 7.1 N, the roll time curve is shown in Figure 18. At 0.329 s, roll is -362.59°, and pitch is 76.9°, which is a perfect flip.

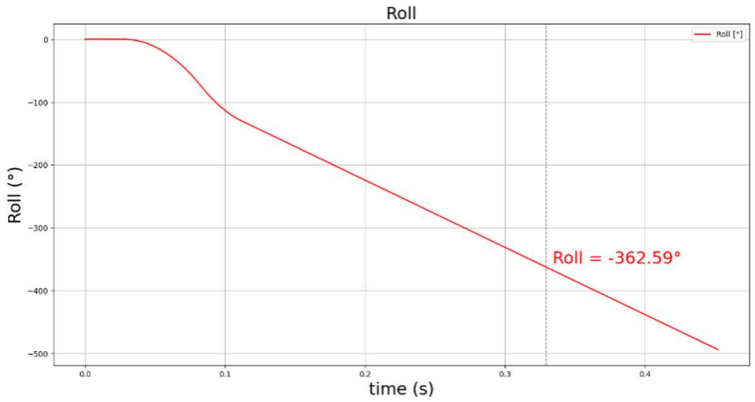

Figure 18. Roll angle over time when flick force F is 7.1 N

From Figure 16, the X coordinate has little effect on roll, so changing X alone cannot achieve a perfect flip. By changing the Y coordinate, it is found that at [89.5, 59.5, 0] (mm), roll at 0.329 s is -352.36°, still not perfect, and Y is already near the short semi-axis limit of 60 mm. Therefore, to achieve a perfect flip by changing the application point, X and Y must be adjusted simultaneously.

When the application point is [69.5, 59.5, 0] (mm), the roll time curve is shown in Figure 19. At 0.329 s, roll is -361.19°, and pitch is 28.2°, which can be regarded as a perfect flip.

Comparing adjustment of F magnitude and application point shows that when only changing force magnitude, perfect flip has roll -362.59° and pitch 76.9°. When only changing application point, perfect flip has roll -361.19° and pitch 28.2°. While athletes focus more on roll, pitch should ideally change less to reduce body sway in the air. Therefore, increasing force magnitude more easily changes roll, while adjusting the application point produces a more significant pitch effect.

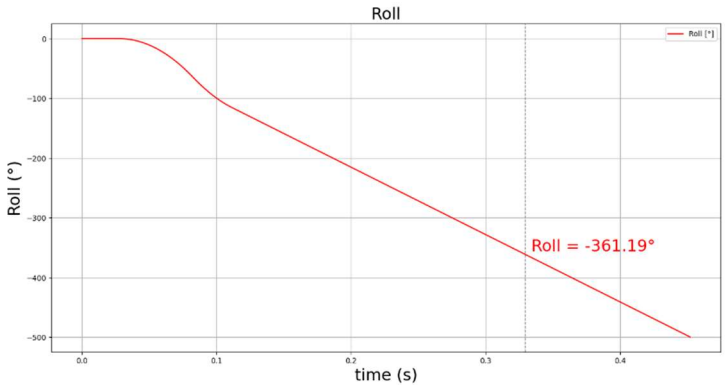

Figure 19. Roll angle over time when application point is [69.5, 59.5, 0]

5. Summary and Outlook

This study focuses on the core skateboard trick KickFlip and proposes a method combining theoretical modeling, simulation, and experimental validation to analyze airborne attitude change after force application. Through rigid-body dynamics derivation, an angular acceleration and attitude evolution model under flick force was established. Combined with an MPU6050 sensor and Arduino, angular velocity and attitude data were obtained to validate the theoretical results.

In experiments, by reasonably selecting the application point, direction, and duration of the flick force, an impulsive force was applied and the flipping process was recorded. The results show that the model has high accuracy in describing the flipping angular velocity and roll change produced about the X axis (skateboard long axis).

Theoretical simulation and experimental data match well, and errors are within an acceptable range, verifying the model's effectiveness.

To further approximate real motion, physical constraints during skateboard contact with the table were modeled, and Y-axis freedom was appropriately constrained, improving the explanation of rotation about the short axis. Also, rebound force analysis enhanced the description of the post-flick rise behavior.

Although initial results have been achieved, several issues remain for deeper study.

(1) Model simplification.

The current model does not consider yaw about the Z axis and neglects friction and air resistance.

(2) Limited experimental conditions.

It is almost impossible to apply the flick force at the instant of free fall, so force was applied at the table edge, which imposes constraints.

(3) Sensor accuracy and algorithm adaptation.

The MPU6050 accelerometer is unstable under high-speed flipping, and yaw has persistent bias due to lack of a magnetometer.

In the future, higher-precision IMU sensors can be introduced, combined with more stable filtering algorithms such as the extended Kalman filter (EKF) or adaptive filtering to further improve attitude estimation quality.

In summary, this study builds a combined theoretical and experimental analysis framework and provides a feasible path for modeling and analyzing skateboard flipping attitude, and the limitations will be continuously explored and improved in future work.

References

[1] https://www.olympics.com/.

[2] Zhang Ping, Liu Zuoshi. Gesture recognition method based on inertial sensor MPU6050. Sensors and Microsystems, 2018, 37(01): 46-49+53.

[3] Yan Li, Shen Mingxia, Yao Wen, et al. Posture recognition method for lactating sows based on MPU6050 sensor. Transactions of the Chinese Society for Agricultural Machinery, 2015, 46(05): 279-285.

[4] Feynman, Leighton, Sands. The Feynman Lectures on Physics. Shanghai: Shanghai Scientific and Technical Publishers, 2020: 102-108.

[5] https://projecthub.arduino.cc/.

[6] Long Jiangteng. Human gesture recognition research based on motion attitude sensor MPU6050. Donghua University of Technology, 2021.

[7] Chen Guoding, Zhou Penghao, Hu Zhenhao, et al. Research on quadrotor hardware attitude estimation based on MPU6050. Mechanical and Electrical Engineering, 2018, 35(01): 95-100.